Alzheimer's & Dementia: Diagnosis, Assessment & Disease Monitoring 6 (2017) 11-20

PART II. State of the Field: Advances in Neuroimaging from the 2016 Alzheimer's Imaging Consortium

Association between Aβ and tau accumulations and their influence on clinical features in aging and Alzheimer's disease spectrum brains: A [^{11}C]PBB3-PET study

Hitoshi Shimada[a,*], Soichiro Kitamura[a], Hitoshi Shinotoh[a,b], Hironobu Endo[a,c], Fumitoshi Niwa[a,d], Shigeki Hirano[a,e], Yasuyuki Kimura[a], Ming-Rong Zhang[f], Satoshi Kuwabara[e], Tetsuya Suhara[a], Makoto Higuchi[a]

[a]*Department of Functional Brain Imaging Research (DOFI), Clinical Research Cluster, National Institute of Radiological Sciences (NIRS), National Institutes for Quantum and Radiological Science and Technology (QST), Chiba-shi, Chiba, Japan*
[b]*Neurology Chiba Clinic, Chiba-shi, Chiba, Japan*
[c]*Division of Neurology, Kobe University Graduate School of Medicine, Kobe-shi, Hyogo, Japan*
[d]*Department of Neurology, Kyoto Prefectural University of Medicine, Kyoto-shi, Kyoto, Japan*
[e]*Department of Neurology, Graduate School of Medicine, Chiba University, Chiba-shi, Chiba, Japan*
[f]*Department of Radiopharmaceuticals Development, Clinical Research Cluster, NIRS, QST, Chiba-shi, Chiba, Japan*

Abstract

Introduction: Amyloid-β (Aβ) and tau accumulations may occur independently and concurrently as exemplified by primary age-related tauopathy and Alzheimer's disease (AD), respectively. Interactions between Aβ and tau accumulations and their influence on clinical features, however, are still unclear.
Methods: Associations among clinical symptoms, gray-matter volume, regional tau, and Aβ deposition assessed by positron emission tomography with [^{11}C]pyridinyl-butadienyl-benzothiazole 3 (PBB3) and [^{11}C]Pittsburgh compound-B (PiB), were evaluated in 17 AD, 9 mild cognitive impairment due to AD, and 28 PiB(−)-cognitive healthy controls (HCs).
Results: High tau burden was associated with aging and low-level education in PiB(−)-HC and AD-spectrum groups, and with high Aβ burden and low-level education in all subjects. It was not Aβ but tau accumulation that showed significant associations with cognitive performance even in PiB(−)-HC.
Discussion: The present study indicated aging and low-level education after Aβ would be enhancers for tau pathology, associated with neurodegeneration and cognitive impairment in healthy and diseased elderly individuals.

Keywords: Tau; Amyloid; Brain atrophy; Cognitive decline; Biomarkers; Alzheimer's disease; MCI; Preclinical; Dementia; Aging; Cognitive reserve; Positron emission tomography; [^{11}C]PBB3; [^{11}C]PiB

1. Introduction

Senile plaques and fibrillary tau inclusions are neuropathological hallmarks of Alzheimer's disease (AD) [1]. As represented by the "amyloid cascade" hypothesis [2], one of the most accepted models of the pathogenesis of AD, it has been considered by many that amyloid-β (Aβ) plays key roles in disease initiation and progression and that it would be a promising target for therapy and imaging. In fact, Aβ imaging by positron emission tomography (PET) has brought about major developments in dementia research and clinical trials. Aβ imaging enables us to make accurate differential

*Corresponding author. Tel.: +81-43-263-8555; Fax: +81-43-253-0396.
E-mail address: shimada.hitoshi@qst.go.jp

http://dx.doi.org/10.1016/j.dadm.2016.12.009

diagnosis [3,4], predict disease progression [5], build a better understanding of the pathogenesis [6–9], and evaluate therapeutic efficacies in clinical trials [10,11]. It remains unclear, however, whether Aβ pathology itself shows neurotoxicity in vivo and influences clinical features. Only a few studies have indicated significant associations between Aβ burden and clinical features in AD [12–14]. Furthermore, recent neuroimaging and neuropathological studies have revealed that some cognitively healthy elderly have abundant neocortical Aβ [15–18].

Tau pathology sometimes occurs concurrently (e.g., AD) with, and sometimes independently (e.g., non-AD tauopathies such as progressive supranuclear palsy, corticobasal degeneration, and primary age-related tauopathy (PART)) of Aβ [19,20]. Accumulating evidence has suggested that tau pathology has a close relation with neurodegeneration equal to or rather than Aβ pathology [21–23]. To assess the effect of tau pathology on neurodegeneration, previous studies had to use animal models, estimate from cerebrospinal fluid (CSF), or wait for postmortem autopsy. These approaches, however, have several limitations. In other words, specific differences, lack of information on location, and temporal interval between autopsy and clinical evaluation make it difficult to evaluate the effect of tau pathology on the human brain environment.

There has been a conspicuous progress in the development of PET agents for tau pathology, as exemplified by [^{18}F]AV-1451 (also known as [^{18}F]T807), [^{18}F]THK-5117, and [^{18}F]THK-5351 [24–26], along with our tau-binding ligand, [^{11}C]pyridinyl-butadienyl-benzothiazole 3 ([^{11}C]PBB3) [27]. Previous studies showed that tau PET imaging using these ligands were able to detect tau pathologies with high sensitivity and specificity even at an early stage and that those signals could reflect the disease severity [24,25,27]. In our present study, we could evaluate tau pathology as well as Aβ with PET imaging quantitatively with spatial information in vivo, together with clinical evaluation.

To elucidate the interaction between Aβ and tau accumulations and their influence on clinical features such as brain atrophy and cognitive decline, we performed a cross-sectional PET study using [^{11}C]PBB3 and [^{11}C]PiB for tau and Aβ imaging, respectively, in both cognitively healthy individuals and patients with cognitive impairments. We also performed voxel-based morphometry using three-dimensional T1-weighted magnetic resonance imaging (MRI) and psychological batteries for assessing brain atrophy and cognitive decline.

2. Methods

2.1. Participants

Clinically diagnosed patients with mild cognitive impairment (MCI) and AD were recruited from Chiba University Hospital and affiliated hospitals between July, 2011 and March, 2014. Clinical diagnoses of AD and MCI were based on the National Institute of Neurological and Communicative Disease and Stroke/Alzheimer's Disease and Related Disorders Association criteria [28] and Petersen's criteria [29], respectively. Cognitive healthy controls (HCs), consisting of age-matched old (oHC) and young (yHC) subjects under or equal to 40 years old as a reference standard group in evaluations of tau and Aβ accumulations, without a history of neurologic and psychiatric disorders, were also recruited from the volunteer association of the National Institute of Radiological Sciences (NIRS), and were without abnormalities in physical and neurological examinations. Because we intended to focus on the aging and AD-spectrum group, PiB(−) patients with dementia, patients with possible and probable dementia with Lewy bodies, six PiB(−) patients with MCI whose pathological backgrounds were expected to be heterogeneous and were excluded from the assay group. Two PiB(+) HCs were also excluded from the further analyses because of its small sample size.

Subjects underwent psychological evaluations including Mini–Mental State Examination (MMSE), clinical dementia rating (CDR) scale, and Wechsler memory scale revised logical memory II (WMSR LM-II) tests for assessing cognitive and functional impairment, Raven's colored progressive matrices (RCPMs) for assessing nonverbal cognitive impairment, and frontal assessment battery (FAB) for evaluating frontal dysfunction.

Written informed consent was obtained from all participants and from spouses or other close family members when the participants were cognitively impaired. This study was approved by the institutional review board of NIRS, in accordance with the ethical code of NIRS and the ethical guidelines for clinical studies of the Ministry of Health, Labour and Welfare in Japan, as well as the Declaration of Helsinki. The study was registered with UMIN Clinical Trials Registry (UMIN-CTR; number 000009863).

2.2. PET data acquisition

[^{11}C]PBB3 and [^{11}C]PiB were produced as previously reported [27,30,31]. PET images were acquired with a Siemens ECAT EXACT HR+ scanner (CTI PET Systems, Inc., Knoxville, TN) with an axial field of view of 155 mm, providing 63 contiguous 2.46-mm slices with 5.6-mm transaxial and 5.4-mm axial resolution. For tau and Aβ imaging, 70-minute dynamic PET scans in three-dimensional mode were performed after an intravenous injection of [^{11}C]PBB3 (432 ± 59 MBq, specific activity 98 ± 51 GBq/μmol) or [^{11}C]PiB (381 ± 29 MBq, specific activity 83 ± 51 GBq/μmol), respectively, on the same day as MRI. [^{11}C]PBB3 was injected in a dimly lit condition to avoid its photoracemization [27,30]. Subjects were examined with their eyes closed and their ears unplugged in a quiet room, and their heads were restrained with a band extending across the forehead attached to the headrest. An examiner carefully monitored head

movement with laser beams during each scan to correct their head positions in case of movement.

All PET images were reconstructed by filtered back-projection method (Hanning filter, cut-off frequency: 0.4 cycle/pixel). Attenuation and scatter corrections were applied for each image using a 10-minute transmission scan with a 68Ge-68Ga line source and single-scatter simulation method, respectively. Atrophy correction was not performed in the present study.

2.3. MRI acquisition

All MRI examinations were performed with a 3-Tesla magnetic resonance scanner (Signa HDx, GE Healthcare, WI, USA, or MAGNETOM Verio, Siemens Healthcare, Erlangen, Germany) on the same day as the [^{11}C]PBB3-PET scan. Three-dimensional volumetric acquisition of a three-dimensional T1-weighted gradient echo sequence (repetition time range/echo time range, 7 ms/2.8 ms; field of view [frequency × phase], 260 mm × 244 mm; matrix, 256 mm × 256 mm; 170 contiguous axial slices of 1.0 mm thickness).

2.4. PET and MRI data analyses

All images were preprocessed using PMOD software version 3.5 (PMOD Technologies Ltd., Zürich, Switzerland) and the Statistical Parametric Mapping software (SPM12, Wellcome Department of Cognitive Neurology, London, UK), operating in the MATLAB software environment (version 7.11; MathWorks, Natick, MA, USA). At first, motion correction was applied for all PET images. Afterward, each PET image was coregistered to individual T1-weighted magnetic resonance images and anatomically normalized (MNI152 standard space, Montreal Neurological Institute, Montreal, QC, Canada) using Diffeomorphic Anatomical Registration Through Exponentiated Lie Algebra (DARTEL) [32].

Parametric [^{11}C]PBB3- and [^{11}C]PiB-PET images were generated by voxel-based calculation of standard uptake value ratio (SUVR) to the cerebellar cortex at 30–50 minutes and 50–70 minutes after the injections, respectively. To estimate mean cortical tau and Aβ burden of each subject, a mean cortical template volume of interest was created consisting of bilateral frontal, medial and lateral temporal, parietal, and occipital cortices using the automated anatomical labeling (AAL) atlas implemented in the Wake Forest University PickAtlas version 2.4 [33] and modified to be devoid of CSF space using CSF maps generated from individual magnetic resonance images.

In the present study, all participants were classified into PiB(+) and PiB(−) using the cutoff value (mean cortical SUVR of [^{11}C]PiB-PET = 1.34), which can maximize the sum of sensitivity and specificity for discrimination between HC and AD. We also visually confirmed that there was no evident [^{11}C]PiB uptake to suggest that Aβ deposition was observed even in any focal region of PiB(−) subjects and that all PiB(+) subjects had abundant uptake of [^{11}C]PiB in their cortex according to the standard method using in the Japanese Alzheimer's Disease Neuroimaging Initiative study. Subsequently, we performed voxel-based correlation analyses to assess the relationship between [^{11}C]PBB3 or [^{11}C]PiB SUVR and MMSE, CDR Sum of Boxes (CDR-SOB), RCPM, or FAB score among the AD-spectrum group. Because WMSR LM-II scores were 0 in most AD-spectrum patients, we perform voxel-based correlation analyses to assess the relationship between [^{11}C]PBB3 or [^{11}C]PiB SUVR and WMSR LM-II score only among PiB(−)-oHC (oHC−) subjects.

2.5. Voxel-based morphometry

Each 3D T1-weighted MRI was segmented and normalized using the unified segmentation approach [34,35] and DARTEL algorithm [32] implemented in SPM12. First, we estimated each whole-brain gray-matter volume (GMV) adjusted by total intracranial volume calculated using native-space tissue maps of each subject. For the purpose of confirming whether the alteration of GMV was associated with tau, Aβ, age, gender, and years of schooling or not, multiple regression analyses were performed in both the AD-spectrum and HC groups.

Second, we also performed voxel-based morphometry analysis, and regions in which GMV was significantly reduced in the AD-spectrum group, compared to the oHC− group, were estimated. Afterward, we confirmed whether regions in which GMV was significantly reduced, compared to the oHC− group, in the AD-spectrum group overlapped with regions in which PBB3/PiB SUVRs were significantly increased, compared to the yHC group.

2.6. Statistical analyses

Statistical analyses were performed using Statistical Package for the Social Sciences software (IBM SPSS version 22, IBM Inc., NY, USA). Group comparisons in demographic variables among the yHC, oHC−, and AD-spectrum groups were implemented by Fisher exact test (gender and CDR), one-way analysis of variance (ANOVA) followed by Bonferroni post hoc test (age), and Kruskal-Wallis one-way ANOVA (years of schooling, MMSE, FAB, WMSR LM-II, RCPM, and CDR sum of boxes). We performed stepwise linear regression analysis to formulate the relation between tau/Aβ burden/GMV and other variables of interests. All P values are indicated on the figures or in the corresponding legends (the level is .05 for all statistical analyses).

3. Results

3.1. Demographic profiles of participants

Demographic and clinical profiles of the participants are summarized in Table 1. Although the yHC group was significantly younger compared to the PiB(−)-oHC and AD-spectrum groups (both $P < .001$), there was no

Table 1
Demographic and neuropsychological test results of participants

	PiB(−)-HC group		AD-spectrum group	
Demographics	yHC	oHC−	MCI+	AD
Number of subjects	10	18	9	17
Gender (male:female)	4:6	12:6	5:4	5:12
Age	38.2 ± 4.7	67.3 ± 6.4	74.2 ± 4.4	71.6 ± 9.6
Years of schooling	15.3 ± 1.3	14.6 ± 1.9	13.2 ± 2.0	10.8 ± 1.8
MMSE	29.5 ± 0.5	28.9 ± 1.2	26.6 ± 2.0	16.1 ± 5.1
FAB	17.2 ± 0.8	17.2 ± 0.9	15.0 ± 1.7	11.3 ± 3.0
WMSR logical memory II	21.7 ± 7.3	15.4 ± 6.3	05.2 ± 7.5	00.2 ± 0.5
CDR sum of boxes	0.0 ± 0.0	00.0 ± 0.1	01.8 ± 0.8	05.9 ± 2.0
CDR				
0	10 (100%)	21 (100%)	-	-
0.5	-	-	9 (100%)	7 (41%)
1	-	-	-	8 (47%)
2	-	-	-	2 (12%)
3	-	-	-	-
Mean cortical SUVR of [^{11}C]PBB3-PET	0.84 ± 0.04	0.91 ± 0.06	0.96 ± 0.05	1.10 ± 0.07
Mean cortical SUVR of [^{11}C]PiB PET	1.11 ± 0.06	1.16 ± 0.08	1.91 ± 0.24	1.92 ± 0.36

Abbreviations: AD, Alzheimer's disease; yHC, young healthy control (HC); oHC−, PiB(−) old HC; MCI+, PiB(+) mild cognitive impairment; MMSE, Mini–Mental State Examination; FAB, frontal assessment battery; WMSR, Wechsler memory scale revised; CDR, clinical dementia rating; SUVR, standard uptake value ratio; [^{11}C]PBB3, [^{11}C]pyridinyl-butadienyl-benzothiazole 3.

NOTE: Values are listed as mean ± SD.

significant difference in age between the PiB(−)-oHC and AD-spectrum groups (P = .200). There was no significant difference in gender among the groups (P = .187). The AD-spectrum group showed significantly fewer years of schooling, and more cognitive functions measured by MMSE, RCPM, and FAB were significantly impaired as compared with the other two groups (P < .001). Furthermore, overall clinical deteriorations assessed by CDR-SOB were also significantly increased in the AD-spectrum subjects compared with the other two groups (P < .001).

3.2. Aβ, aging, and lower level education were possible enhancers of tau deposition

Relationships among tau, Aβ, and age were different between the PiB(−)-HC and AD-spectrum groups (Fig. 1). Multiple regression analyses showed that Aβ (standardized coefficient [β] 0.590, standard error [SE] 0.026, P < .001) and years of schooling (β −0.284, SE 0.005, P = .011) were independently associated with mean cortical tau burden in all subjects (adjusted R^2 = 0.626). In addition, multiple regression analyses also showed that age and years of schooling were independently associated with mean cortical tau burden in both the PiB(−)-HC and AD-spectrum groups (age: β 0.476 and −0.507, SE 0.001 and 0.002, P = .004 and 0.021; years of schooling: β −0.391 and −0.448, SE 0.006 and 0.008, P = .015 and 0.040; adjusted R^2 = 0.434 and 0.178, respectively).

3.3. Tau pathology was closely associated with medial temporal atrophy

Relationships between GMV and tau/Aβ burdens are shown in Fig. 2. Multiple regression analyses showed that age (β −0.398, SE 0.000, P < .001), mean cortical tau burdens (β −0.521, SE 0.047, P < .001), and male gender (β −0.245, SE 0.010, P = .007) were negatively associated with adjusted whole GMV in all subjects independently (adjusted R^2 = 0.646). Furthermore, multiple regression analyses also showed that age (β −0.548, SE 0.000, P < .001) and male gender (β −0.487, SE 0.010, P < .001) were negatively associated with adjusted whole GMV in the PiB(−)-HC group independently and that only cortical tau burden (β −0.419, SE 0.033, P = .033) was negatively associated with adjusted whole GMV in the AD-spectrum group independently (R^2 = 0.141).

Voxel-based analyses revealed that GMV was significantly decreased especially around the medial temporal region in the AD-spectrum group compared to the oHC− group, and that PBB3(+)-tau was significantly increased in the widespread neocortex including the medial temporal region. In contrast, PiB(+)-Aβ was less evident around the medial temporal region in spite of significant increase of PiB(+)-Aβ in almost the entire neocortex. Thereafter, to focus on the medial temporal region in which the most characteristic brain atrophy was shown in the AD-spectrum group, we applied the medial temporal mask created by the AAL atlas to SPM analyses assessing changes in GMV, tau, and Aβ. SPM analysis then revealed that brain atrophy well overlapped with brain regions in which PBB3(+)-tau was observed in the AD spectrum (Fig. 3).

3.4. Cognitive deficits were associated with tau, but not with Aβ

In the AD-spectrum group, global cognitive functions evaluated by MMSE and RCPM were inversely correlated

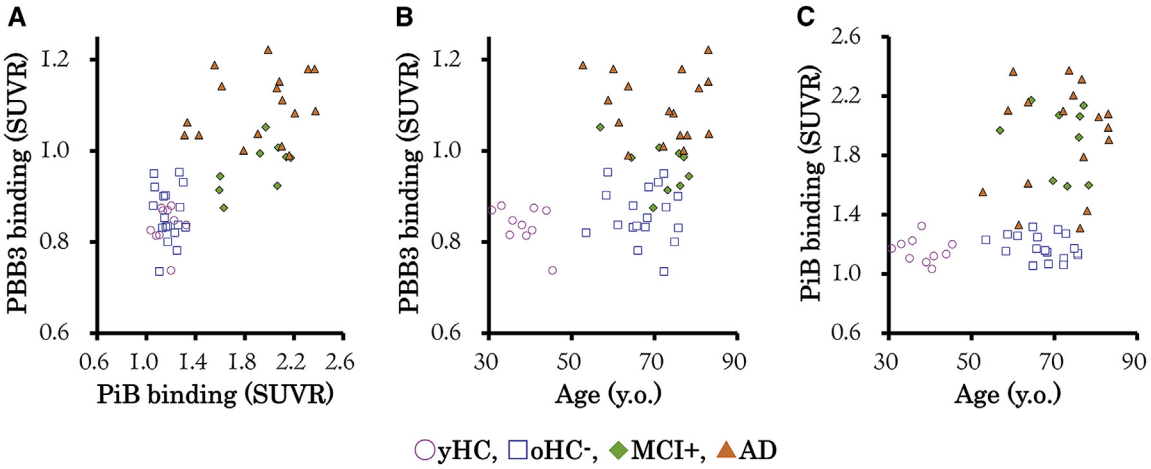

Fig. 1. Associations among mean cortical tau/Aβ burdens and aging. Scatter plots show the association between mean cortical [^{11}C]PBB3 and [^{11}C]PiB bindings (A), between mean cortical [^{11}C]PBB3 binding and age (B), and between mean cortical [^{11}C]PiB3 binding and age (C). Filled and open symbols indicate PiB-positive and PiB-negative subjects, respectively. Spearman correlations (rho) between two variables are as follows. (A) All, $n = 54$, Spearman $\rho = 0.769$, $P < .001$; PiB(−)-HC, $n = 28$, Spearman $\rho = 0.058$, $P = .385$; AD spectrum, $n = 26$, Spearman $\rho = 0.355$, $P = .038$. (B) All, $n = 54$, Spearman $\rho = 0.508$, $P < .001$; PiB(−)-HC, $n = 28$, Spearman $\rho = 0.578$, $P = .001$; AD spectrum, $n = 26$, Spearman $\rho = -0.296$, $P = .071$. (C) All, $n = 54$, Spearman $\rho = 0.452$, $P < .001$; PiB(−)-HC, $n = 28$, Spearman $\rho = 0.368$, $P = .027$; AD spectrum, $n = 26$, Spearman $\rho = -0.143$, $P = .242$. Abbreviations: [^{11}C]PBB3, [^{11}C]pyridinyl-butadienyl-benzothiazole 3; Aβ, amyloid β; AD, Alzheimer's disease; HC, health control; MCI+, PiB(+) mild cognitive impairment; oHC−, PiB(−) old HC; SUVR, standard uptake value ratio; yHC, young healthy control.

with PBB3-positive tau in areas including frontal and temporo-parietal junctions (Fig. 4). Moreover, overall clinical deteriorations assessed by CDR-SOB were positively correlated with PBB3-positive tau in areas including the limbic and paralimbic structures and fronto-parietal cortices (Fig. 4). Furthermore, frontal lobe–associated neuropsychological scales determined by FAB were inversely correlated with PBB3-PET signals in the frontal regions in the AD-spectrum group (Fig. 4), with local maxima of the statistical significance being localized to the medial frontal and anterior cingulate gyri. Meanwhile, no overt relation of PiB(+) Aβ to scores of any psychological batteries was observed in any of the brain areas (data not shown).

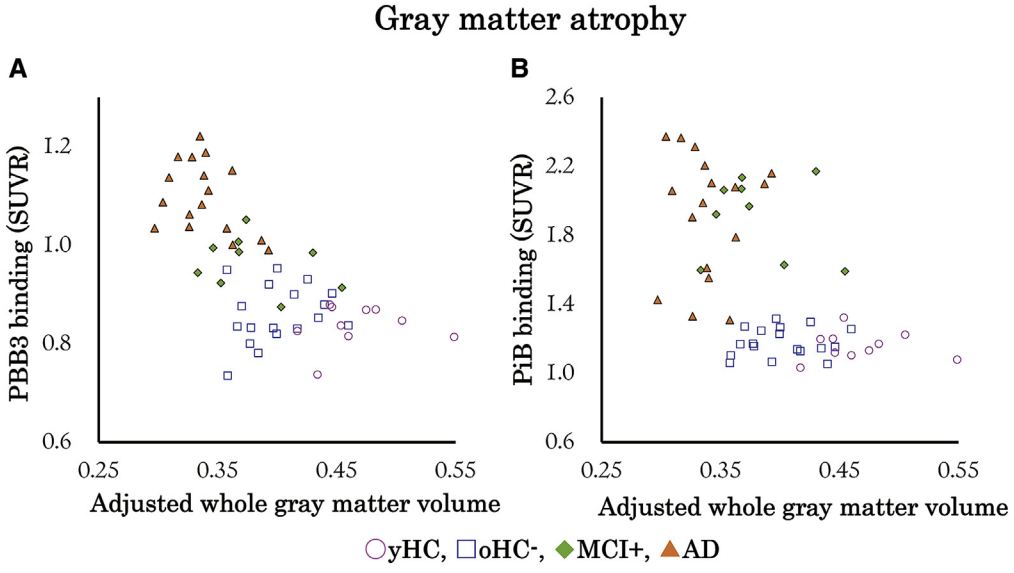

Fig. 2. Association between adjusted whole gray matter and tau/Aβ burdens. Scatter plots show association between whole gray matter adjusted by intracranial volume and mean cortical [^{11}C]PBB3 (A), and between whole gray matter adjusted by intracranial volume and [^{11}C]PiB bindings (B). Filled and open symbols indicate PiB-positive and PiB-negative subjects, respectively. Spearman correlations (rho) between two variables are as follows. (A) All, $n = 54$, Spearman $\rho = -0.667$, $P < .001$; PiB(−)-HC, $n = 28$, Spearman $\rho = -0.275$, $P = .078$; AD spectrum, $n = 26$, Spearman $\rho = -0.419$, $P = .017$. (B) All, $n = 54$, Spearman $\rho = -0.617$, $P < .001$; PiB(−)-HC, $n = 28$, Spearman $\rho = -0.241$, $P = .108$; AD spectrum, $n = 26$, Spearman $\rho = -0.130$, $P = .263$. Abbreviations: [^{11}C]PBB3, [^{11}C]pyridinyl-butadienyl-benzothiazole 3; Aβ, amyloid β; AD, Alzheimer's disease; HC, health control; MCI+, PiB(+) mild cognitive impairment; oHC−, PiB(−) old HC; SUVR, standard uptake value ratio; yHC, young healthy control.

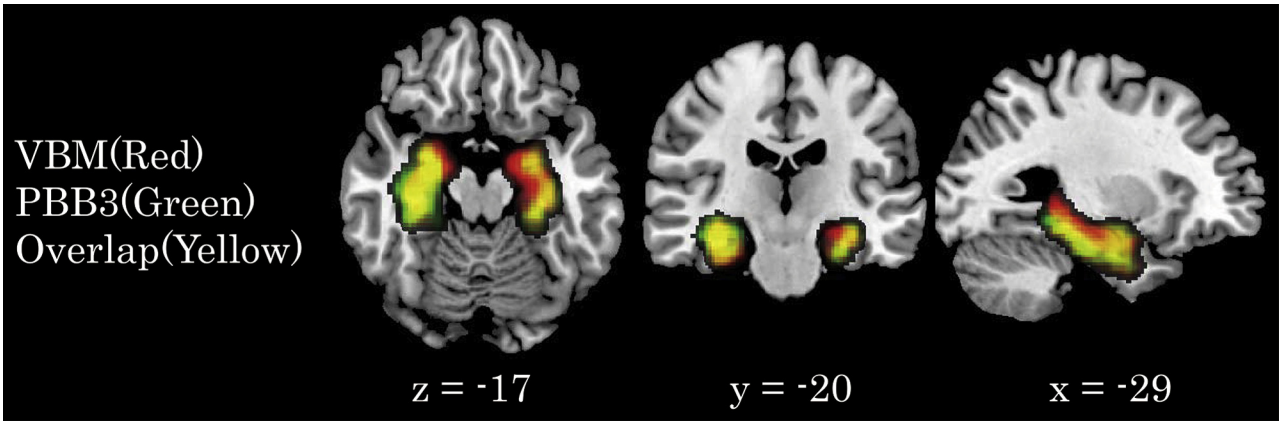

Fig. 3. Comparison between brain atrophy and tau deposition in the medial temporal cortex among the AD spectrum. Statistical parametric maps illustrated brain atrophy and tau deposition in the medial temporal cortex among the AD-spectrum group. Red and green areas indicate regions where a reduction in GMV was observed in the AD-spectrum group compared to the oHC− group, and where an increase in [^{11}C]PBB3 uptake was observed in the AD-spectrum group compared to the yHC group, respectively. Overlapped areas between a reduction in GMV and an increase in [^{11}C]PBB3 uptake are mapped with yellow. Results were expressed in the Montreal Neurological Institute coordinate space. Abbreviations: [^{11}C]PBB3, [^{11}C]pyridinyl-butadienyl-benzothiazole 3; AD, Alzheimer's disease; GMV, gray-matter volume; oHC−, PiB(−) old healthy control; VBM, voxel-based morphometry.

As for the oHC− group, memory functions examined by WMSR LM-II were inversely correlated with deposition of PBB3-detectable tau in the hippocampal formation and several cortical regions. These regions included the left hippocampus/amygdala, left lateral temporal cortex, and right intersectional area among the temporal, parietal, and occipital borders (Fig. 4).

4. Discussion

The present study demonstrated that tau accumulation showed significant positive correlation with Aβ pathology in all subjects. Furthermore, age showed significant positive correlation with tau burden in the PiB(−)-HC group, although brain regions where significant uptake of [^{11}C]PBB3 was observed in the oHC− group compared to the yHC group were in a relatively restricted area around the medial temporal region including parahippocampal structure (Supplementary Fig. 1 and Supplementary Table 1). Previous pathological studies reported that neurofibrillary tangles (NFTs) are frequently observed in aged brain despite the absence of Aβ plaque, especially around the medial temporal lobe. Nowadays, many neuropathologists regard the appearance of tau pathology in aged brains as inevitable, and the new term "PART" has been proposed for such a pathological condition [20]. It is also reported that PART-type pathology generally does not progress to the isocortical Braak stages (i.e., V–VI), remaining in a relatively restricted area. In previous PET studies, Schöll et al. reported that PET detection of tau with [^{18}F]AV-1451 in isocortical regions

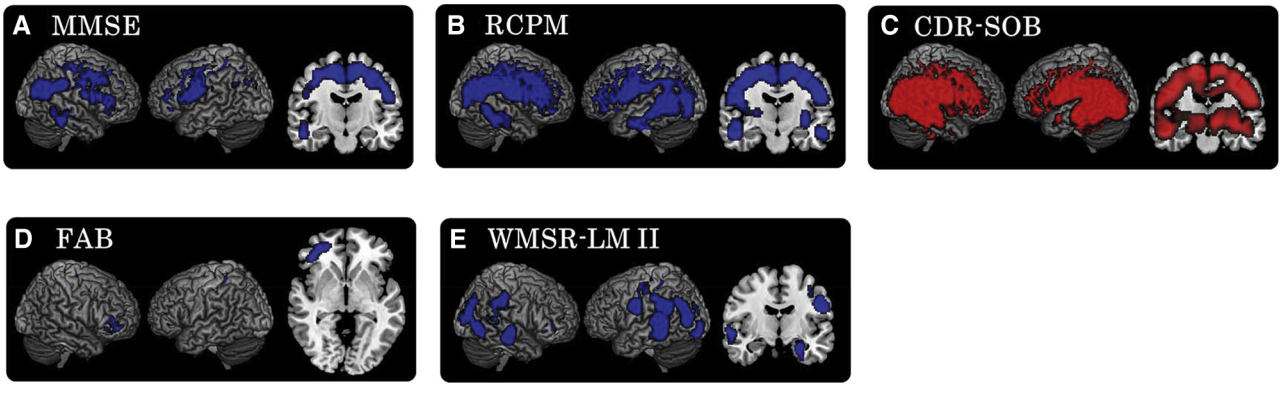

Fig. 4. Voxel-based analyses of correlations between clinical manifestations and tau deposition. Regions with significant correlations of [^{11}C]PBB3 SUVR with (A) MMSE; (B) RCPM; (C) CDR-SOB; (D) FAB among the AD spectrum, and with (E) WMSR LM-II among oHC− are mapped on a standard anatomical space. Blue and red areas indicate regions where negative and positive correlations are shown, respectively. Data are thresholded at false discovery rate–corrected P value $< .05$ and extent threshold >500 voxels (A–C) and at uncorrected P value $< .005$ and extent threshold >200 voxels (D, E), respectively. Abbreviations: [^{11}C]PBB3, [^{11}C]pyridinyl-butadienyl-benzothiazole 3; AD, Alzheimer's disease; FAB, frontal assessment battery; MMSE, Mini–Mental State Examination; oHC−, PiB(−) old healthy control; RCPM, Raven's colored progressive matrix; SUVR, standard uptake value ratio; WMSR LM-II, Wechsler memory scale revised logical memory II.

required the presence of Aβ except the medial temporal lobe [36]. Our results were compatible with previous reports and add further evidence supporting the hypothesis that tau pathology gradually expands in concert with aging within the restricted region around the medial temporal cortex, and that Aβ pathology would make tau pathology expand beyond the collateral sulcus to the entire neocortex as a strong enhancer of tau spreading.

In contrast, age showed significant negative correlation with tau burden in the AD-spectrum subjects. Previous neuropathological study demonstrated that the prevalence of moderate and severe AD-related neuropathological changes, including neuritic plaque and NFT, decreased with increasing age in elderly patients with dementia [37]. Our results corresponded with previous pathological findings. The inverse association between aging and AD-related pathology in elderly patients with dementia would be explained by two possible reasons. First, concomitant mixed pathologies would allow elderly patients with AD show severe clinical symptoms considering their severity of AD-related neuropathological changes are mild. Second, there would be some difference in pathological basis between early- and late-onset AD patients. Previous neuroimaging studies revealed that distribution and progression patterns of brain atrophy were different between early- and late-onset AD patients [38]. Ossenkoppele et al. reported that younger age was associated with greater [^{18}F]AV-1451 increase in wide regions of the neocortex in the AD-spectrum patients, whereas older age was associated with greater uptake of [^{18}F]AV-1451 in the AD-spectrum group [39]. These results would suggest that NFT would arise differently at early- or late-onset AD, leading to different cognitive and neuroimaging profiles.

Interestingly enough, the years of schooling showed a significant negative correlation with tau burden in both the PiB(−)-HC and AD-spectrum groups. To our knowledge, there was no previous report demonstrating significant association between the years of schooling and tau burden assessed by PET. Zhang et al. reported that lower education was associated with a higher prevalence of AD and other dementia [40]. Moreover, some neuropathological studies, as exemplified by the Nun Study [41], revealed that some cognitive healthy elderly have Aβ and tau pathologies in their brain. The concept of cognitive reserve (CR) has been postulated to explain reasons for such influence of education or occupation on the prevalence of dementia and relatively preserved cognitive performance despite their AD-related pathologies [42,43]. Neural reserve and neural compensation are presumed to underlie the mechanism of CR [44,45]. Recent studies demonstrated CR-related changes in cerebral blood flow, brain network, neuronal hypertrophy, CSF biomarker of AD, and Aβ pathology assessed by amyloid PET [43,46–48]. Our results indicated that education could also show a preventive effect on the expansion of tau pathology.

Brain atrophy observed in the AD-spectrum subject is correlated not with Aβ but with tau pathologies. Medial temporal atrophy used to be generally considered as a specific finding for AD; however, recent imaging and pathological studies revealed that medial temporal atrophy is not necessarily specific for AD but rather is generally observed in cognitive healthy elderly or in patients with suspected non-AD pathophysiology (SNAP) [20,49]. Because tau pathology around the medial temporal region is also observed in cognitive healthy elderly with PART of a part of SNAP, it is assumed that tau pathology would also contribute to medial temporal atrophy in this cohort. In the present study, age and male gender were negatively associated with GMB in the PiB(−)-HC. Our results were compatible with previous neuroimaging study [50]; however, neither tau nor Aβ was associated with GMV in the PiB(−)-HC. Previous neuroimaging study also reported that there was no significant association between tau burden assessed by [^{18}F]AV-1451 and brain volume in the hippocampus among Aβ(−) HC [51]. The lack of significant association between tau burden and brain volume in the Aβ(−) HC could be partly due to the small sample size, the relatively younger age of oHC− compared to generally reported subjects with PART, the effect of the background (e.g., *APOE* gene) or pathological changes other than Aβ and tau (e.g., hippocampal sclerosis, TDP-43, hydrocephalus), and so on.

As for the association between cognitive performance and brain pathologies, tau accumulation showed a close relationship with cognitive decline even in the oHC− group as well as the AD-spectrum group, whereas Aβ deposition did not. For example, AD-spectrum patients with high tau accumulations in the frontal area showed severe frontal dysfunction, and oHC− subjects with marked tau accumulations in the parahippocampal area showed profound recent memory disturbance, according to their degree of regional tau burden. Some previous studies also reported that there were close association between clinical impairment and tau burden assessed by PET [36,39,52,53]. Although some exceptions, such as Sister Mary, who was reported in the Nun Study [41], exist, our results support the hypothesis that tau pathology has a pivotal role in neuronal dysfunction and degeneration.

Limitations of the study are the small number of preclinical AD and older oHC− subjects, and a lack of information about the apolipoprotein E genotype. Therefore, further studies are needed to confirm associations among tau pathology, clinical features, and genetic background, especially in subjects with PART and preclinical AD. In terms of technical aspects, lack of partial volume correction and possible off-target binding are also limitations. The first issue could underestimate regional tau and Aβ burdens, leading to false-negative results especially in correlation analyses; however, it would not hamper any positive results presented in the present study. As for the second issue, we reconfirmed

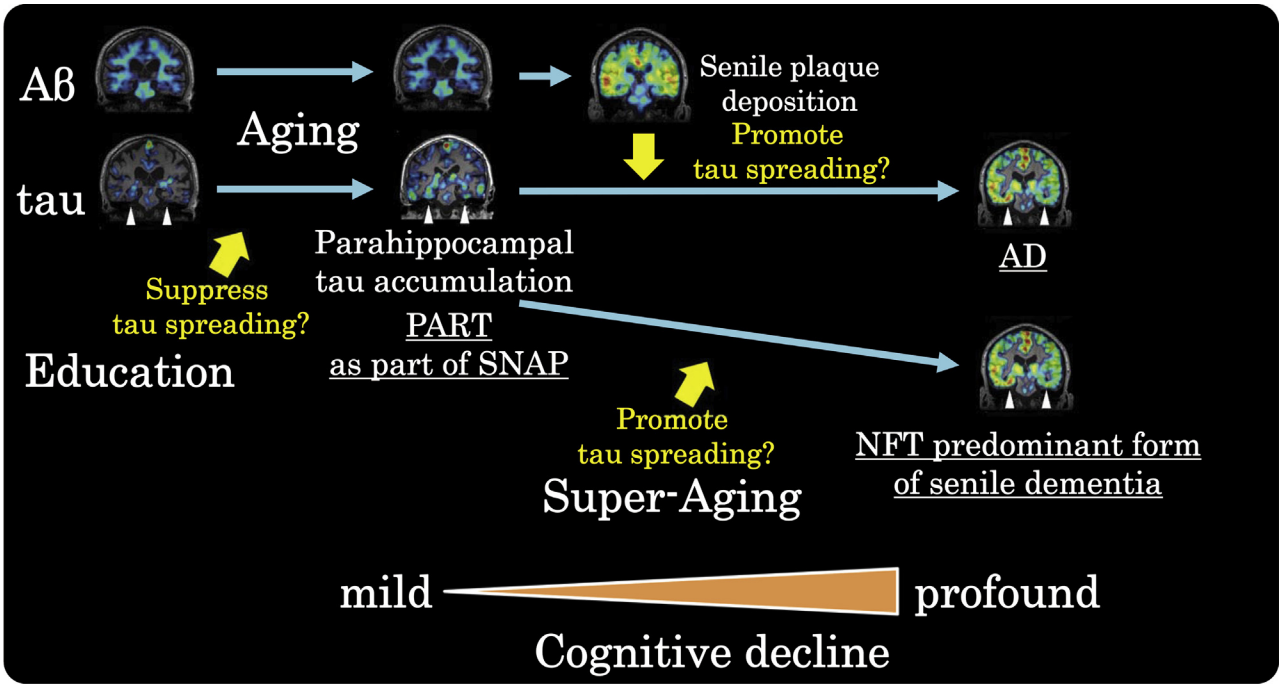

Fig. 5. Hypothetical model of association among aging, education, and Aβ/tau pathologies. Each image is a conceptual tau PET image with [^{11}C]PBB3 overlayed with T1-weighted MRI (coronal slice). Abbreviations: [^{11}C]PBB3, [^{11}C]pyridinyl-butadienyl-benzothiazole 3; Aβ, amyloid β; AD, Alzheimer disease; MRI, magnetic resonance imaging.

our results using brain mask to minimize the spillover effect from extra brain structure such as sinus and choroid plexus.

In conclusion, the current results support the notion of a regional effect of tau pathology on neuronal dysfunction and degeneration in both the AD spectrum and PiB(−)-elderly. Aging together with Aβ pathology would associate with the spreading of tau pathology, whereas education could have a preventive effect on the expansion of tau pathology (Fig. 5). In the absence of super aging, tau pathology in subjects with PART might hardly extend to the neocortex due to a lack of Aβ pathology as a strong enhancer of tau spreading. Oldest-old subjects might show tau expansion to the neocortex despite a lack of Aβ pathology, leading to cognitive decline, and they would be recognized as an NFT-predominant form of senile dementia (Fig. 5). Early intervention against Aβ may prevent or delay a rapid progression of cognitive decline in AD-spectrum patients, although slowly progression of cognitive decline due to aging could occur even after Aβ-targeted intervention without tau-targeting therapy.

Acknowledgments

The authors thank all patients, their caregivers, and volunteers for their participation in the study. The authors also acknowledge the support of K. Takahata, S. Moriguchi, T. Sasaki, H. Fujiwara, F. Kodaka, S. Furukawa, Y. Eguchi, K. Yamaoka, A. Isato, M. Maruyama, H. Takano, I. Kaneko, K. Suzuki, J. Ichikawa, S. Kawakami, Y. Toyota, M. Kurokawa, A. Kurose, Y. Iwasawa, and the radiochemistry staffs and radiological technologists at NIRS (no particular order). The authors acknowledge support for the recruitment of patients with cognitive decline of Y. Yoshiyama at the Inage Neurology and Memory Clinic, K. Kashiwado at Kashiwado Hospital, and K.Suzuki at the Shirogane Orthopedics Clinic.

This work was partly supported by grants from Grants-in-Aid for the Brain Mapping by Integrated Neurotechnologies for Disease Studies (Brain/MINDS; 15653129) to T.S. and M.H. and Research and Development Grants for Dementia (16768966) to M.H. from the Japan Agency for Medical Research and Development; the Japan Advanced Molecular Imaging Program and the Mochida Memorial Foundation for Medical Pharmaceutical Research to H.S.; the Life Science Foundation of Japan to H.S.; the Kashiwado Memorial Foundation to H.S.; the young scientists (A) (26713031) to H.S.; and Scientific Research on Innovative Areas ("Brain Environment" 23111009 to M.H., and "Brain Protein Aging" 26117001 to N.S.) from the Ministry of Education, Culture, Sports, Science and Technology, Japan. H.S., M.-R.Z., T.S., and M.H. hold a patent on compounds related to the present report (JP 5422782/EP 12 884 742.3).

Supplementary data

Supplementary data related to this article can be found at http://dx.doi.org/10.1016/j.dadm.2016.12.009.

RESEARCH IN CONTEXT

1. Systematic review: To investigate interactions between amyloid-β (Aβ) and tau accumulations and their influence on clinical features in Alzheimer's disease (AD) spectrum patients and aging subjects, we performed a cross-sectional PET study using [^{11}C]PBB3 and [^{11}C]PiB for tau and Aβ imaging, along with structural magnetic resonance imaging and psychological batteries.
2. Interpretation: Tau accumulation was significantly associated with cognitive performance even in PiB(−)-healthy control (HC). By contrast, Aβ accumulation did not show any significant correlation with cognitive decline. Multiple regression analyses revealed that high tau burden was associated with aging and low-level education in the PiB(−)-HC and AD groups, and with high Aβ burden and low-level education in all subjects, respectively.
3. Future direction: Our results suggest that aging in parallel with Aβ pathology would be an enhancer of expanding tau pathology and that cognitive reserve might be partly based on the suppression of tau pathology. Further longitudinal studies with large sample sizes are needed.

References

[1] Trojanowski JQ, Lee VM. "Fatal attractions" of proteins. A comprehensive hypothetical mechanism underlying Alzheimer's disease and other neurodegenerative disorders. Ann N Y Acad Sci 2000;924:62–7.

[2] Hardy JA, Higgins GA. Alzheimer's disease: the amyloid cascade hypothesis. Science 1992;256:184–5.

[3] Bensaïdane MR, Beauregard JM, Poulin S, Buteau FA, Guimond J, Bergeron D, et al. Clinical utility of amyloid PET imaging in the differential diagnosis of atypical dementias and its impact on caregivers. J Alzheimers Dis 2016;52:1251–62.

[4] Sha SJ, Ghosh PM, Lee SE, Corbetta-Rastelli C, Jagust WJ, Kornak J, et al. Predicting amyloid status in corticobasal syndrome using modified clinical criteria, magnetic resonance imaging and fluorodeoxyglucose positron emission tomography. Alzheimers Res Ther 2015;7:8.

[5] Okello A, Koivunen J, Edison P, Archer HA, Turkheimer FE, Någren K, et al. Conversion of amyloid positive and negative MCI to AD over 3 years: An 11C-PIB PET study. Neurology 2009;73:754–60.

[6] Sperling RA, Laviolette PS, O'Keefe K, O'Brien J, Rentz DM, Pihlajamaki M, et al. Amyloid deposition is associated with impaired default network function in older persons without dementia. Neuron 2009;63:178–88.

[7] Jack CR Jr, Knopman DS, Jagust WJ, Shaw LM, Aisen PS, Weiner MW, et al. Hypothetical model of dynamic biomarkers of the Alzheimer's pathological cascade. Lancet Neurol 2010;9:119–28.

[8] Shimada H, Shinotoh H, Hirano S, Miyoshi M, Sato K, Tanaka N, et al. β-Amyloid in Lewy body disease is related to Alzheimer's disease-like atrophy. Mov Disord 2013;28:169–75.

[9] Villemagne VL, Burnham S, Bourgeat P, Brown B, Ellis KA, Salvado O, et al., Australian Imaging Biomarkers and Lifestyle (AIBL) Research Group. Amyloid β deposition, neurodegeneration, and cognitive decline in sporadic Alzheimer's disease: a prospective cohort study. Lancet Neurol 2013;12:357–67.

[10] Liu E, Schmidt ME, Margolin R, Sperling R, Koeppe R, Mason NS, et al. Bapineuzumab 301 and 302 Clinical Trial Investigators. Amyloid-β 11C-PiB-PET imaging results from 2 randomized bapineuzumab phase 3 AD trials. Neurology 2015;85:692–700.

[11] Sevigny J, Chiao P, Bussière T, Weinreb PH, Williams L, Maier M, et al. The antibody aducanumab reduces Aβ plaques in Alzheimer's disease. Nature 2016;537:50–6.

[12] Frisoni GB, Lorenzi M, Caroli A, Kemppainen N, Någren K, Rinne JO. In vivo mapping of amyloid toxicity in Alzheimer disease. Neurology 2009;72:1504–11.

[13] Marshall GA, Donovan NJ, Lorius N, Gidicsin CM, Maye J, Pepin LC, et al. Apathy is associated with increased amyloid burden in mild cognitive impairment. J Neuropsychiatry Clin Neurosci 2013;25:302–7.

[14] Mori T, Shimada H, Shinotoh H, Hirano S, Eguchi Y, Yamada M, et al. Apathy correlates with prefrontal amyloid β deposition in Alzheimer's disease. J Neurol Neurosurg Psychiatry 2014;85:449–55.

[15] Katzman R, Terry R, DeTeresa R, Brown T, Davies P, Fuld P, et al. Clinical, pathological, and neurochemical changes in dementia: a subgroup with preserved mental status and numerous neocortical plaques. Ann Neurol 1988;23:138–44.

[16] Rowe CC, Ng S, Ackermann U, Gong SJ, Pike K, Savage G, et al. Imaging beta-amyloid burden in aging and dementia. Neurology 2007;68:1718–25.

[17] Price JL, McKeel DW Jr, Buckles VD, Roe CM, Xiong C, Grundman M, et al. Neuropathology of nondemented aging: presumptive evidence for preclinical Alzheimer disease. Neurobiol Aging 2009;30:1026–36.

[18] Quigley H, Colloby SJ, O'Brien JT. PET imaging of brain amyloid in dementia: a review. Int J Geriatr Psychiatry 2011;26:991–9.

[19] Higuchi M, Lee VM, Trojanowski JQ. Tau and axonopathy in neurodegenerative disorders. Neuromolecular Med 2002;2:131–50.

[20] Crary JF, Trojanowski JQ, Schneider JA, Abisambra JF, Abner EL, Alafuzoff I, et al. Primary age-related tauopathy (PART): a common pathology associated with human aging. Acta Neuropathol 2014;128:755–66.

[21] Arriagada PV, Growdon JH, Hedley-Whyte ET, Hyman BT. Neurofibrillary tangles but not senile plaques parallel duration and severity of Alzheimer's disease. Neurology 1992;42:631–9.

[22] Nelson PT, Alafuzoff I, Bigio EH, Bouras C, Braak H, Cairns NJ, et al. Correlation of Alzheimer disease neuropathologic changes with cognitive status: a review of the literature. J Neuropathol Exp Neurol 2012;71:362–81.

[23] van Rossum IA, Vos SJ, Burns L, Knol DL, Scheltens P, Soininen H, et al. Injury markers predict time to dementia in subjects with MCI and amyloid pathology. Neurology 2012;79:1809–16.

[24] Chien DT, Bahri S, Szardenings AK, Walsh JC, Mu F, Su MY, et al. Early clinical PET imaging results with the novel PHF-tau radioligand [F-18]-T807. J Alzheimers Dis 2013;34:457–68.

[25] Ishiki A, Okamura N, Furukawa K, Furumoto S, Harada R, Tomita N, et al. Longitudinal assessment of tau pathology in patients with Alzheimer's disease using [18F]THK-5117 positron emission tomography. PLoS One 2015;10:e0140311.

[26] Lockhart SN, Baker SL, Okamura N, Furukawa K, Ishiki A, Furumoto S, et al. Dynamic PET measures of tau accumulation in cognitively normal older adults and Alzheimer's disease patients measured using [18F] THK-5351. PLoS One 2016;11:e0158460.

[27] Maruyama M, Shimada H, Suhara T, Shinotoh H, Ji B, Maeda J, et al. Imaging of tau pathology in a tauopathy mouse model and in Alzheimer patients compared to normal controls. Neuron 2013;79:1094–108.

[28] McKhann G, Drachman D, Folstein M, Katzman R, Price D, Stadlan EM. Clinical diagnosis of Alzheimer's disease: report of the

NINCDS-ADRDA Work Group under the auspices of Department of Health and Human Services Task Force on Alzheimer's Disease. Neurology 1984;34:939–44.
[29] Petersen RC, Smith GE, Waring SC, Ivnik RJ, Tangalos EG, Kokmen E. Mild cognitive impairment: clinical characterization and outcome. Arch Neurol 1999;56:303–8.
[30] Hashimoto H, Kawamura K, Igarashi N, Takei M, Fujishiro T, Aihara Y, et al. Radiosynthesis, photoisomerization, biodistribution, and metabolite analysis of 11C-PBB3 as a clinically useful PET probe for imaging of tau pathology. J Nucl Med 2014;55:1532–8.
[31] Kimura Y, Ichise M, Ito H, Shimada H, Ikoma Y, Seki C, et al. Quantification of tau pathology in human brain with 11C-PBB3. J Nucl Med 2015;56:1359–65.
[32] Ashburner J. A fast diffeomorphic image registration algorithm. Neuroimage 2007;38:95–113.
[33] Maldjian JA, Laurienti PJ, Kraft RA, Burdette JH. An automated method for neuroanatomic and cytoarchitectonic atlas-based inter- rogation of fMRI data sets. Neuroimage 2003;19:1233–9.
[34] Ashburner J, Friston KJ. Voxel-based morphometry—the methods. Neuroimage 2000;11:805–21.
[35] Ashburner J, Friston KJ. Unified segmentation. Neuroimage 2005; 26:839–51.
[36] Schöll M, Lockhart SN, Schonhaut DR, O'Neil JP, Janabi M, Ossenkoppele R, et al. PET imaging of tau deposition in the aging human brain. Neuron 2016;89:971–82.
[37] Savva GM, Wharton SB, Ince PG, Forster G, Matthews FE, Brayne C. Medical Research Council Cognitive Function and Ageing Study. Age, neuropathology, and dementia. N Engl J Med 2009;360:2302–9.
[38] Migliaccio R, Agosta F, Possin KL, Canu E, Filippi M, Rabinovici GD, et al. Mapping the Progression of Atrophy in Early- and Late-Onset Alzheimer's Disease. J Alzheimers Dis 2015;46:351–64.
[39] Ossenkoppele R, Schonhaut DR, Schöll M, Lockhart SN, Ayakta N, Baker SL, et al. Tau PET patterns mirror clinical and neuroanatomical variability in Alzheimer's disease. Brain 2016;139:1551–67.
[40] Zhang M, Katzman R, Salmon D, Jin H, Cai G, Wang Z, et al. The prevalence of dementia and Alzheimer's disease in Shanghai, China: impact of age, gender and education. Ann Neurol 1990;27:428–37.
[41] Snowdon DA. Aging and Alzheimer's disease: lessons from the Nun Study. Gerontologist 1997;37:150–6.
[42] Stern Y. What is cognitive reserve? Theory and research application of the reserve concept. J Int Neuropsychol Soc 2002;8:448–60.
[43] Stern Y. Cognitive reserve in ageing and Alzheimer's disease. Lancet Neurol 2012;11:1006–12.
[44] Stern Y. Cognitive reserve. Neuropsychologia 2009;47:2015–28.
[45] Stern Y, Habeck C, Moeller J, Scarmeas N, Anderson KE, Hilton HJ, et al. Brain networks associated with cognitive reserve in healthy young and old adults. Cereb Cortex 2005;15:394–402.
[46] Iacono D, Markesbery WR, Gross M, Pletnikova O, Rudow G, Zandi P, et al. The Nun study: clinically silent AD, neuronal hypertrophy, and linguistic skills in early life. Neurology 2009;73:665–73.
[47] Almeida RP, Schultz SA, Austin BP, Boots EA, Dowling NM, Gleason CE, et al. Effect of cognitive reserve on age-related changes in cerebrospinal fluid biomarkers of Alzheimer disease. JAMA Neurol 2015;72:699–706.
[48] Baucknehtt M, Picco A, Nobili F, Morbelli S. Amyloid positron emission tomography and cognitive reserve. World J Radiol 2015; 7:475–83.
[49] Jack CR Jr, Knopman DS, Chételat G, Dickson D, Fagan AM, Frisoni GB, et al. Suspected non-Alzheimer disease pathophysiology—concept and controversy. Nat Rev Neurol 2016; 12:117–24.
[50] Good CD, Johnsrude IS, Ashburner J, Henson RN, Friston KJ, Frackowiak RS. A voxel-based morphometric study of ageing in 465 normal adult human brains. Neuroimage 2001;14:21–36.
[51] Wang L, Benzinger TL, Su Y, Christensen J, Friedrichsen K, Aldea P, et al. Evaluation of tau imaging in staging Alzheimer disease and revealing interactions between β-amyloid and tauopathy. JAMA Neurol 2016;73:1070–7.
[52] Johnson KA, Schultz A, Betensky RA, Becker JA, Sepulcre J, Rentz D, et al. Tau positron emission tomographic imaging in aging and early Alzheimer disease. Ann Neurol 2016;79:110–9.
[53] Brier MR, Gordon B, Friedrichsen K, McCarthy J, Stern A, Christensen J, et al. Tau and Aβ imaging, CSF measures, and cognition in Alzheimer's disease. Sci Transl Med 2016;8:338ra66.